Available online at www.sciencedirect.com
ScienceDirect
Journal of Solid State Chemistry 180 (2007) 1998–2003
JOURNAL OF SOLID STATE CHEMISTRY
www.elsevier.com/locate/jssc

Compressibilities of disordered fluoride pyrochlores $NaCdZn_2F_7$ and $NaCaMg_2F_7$

Andrzej Grzechnik[a,*], Jose Maria Posse[a], Wolfgang Morgenroth[b,c], Karen Friese[a]

[a]*Departamento de Física de la Materia Condensada, Universidad del País Vasco, Bilbao, Spain*
[b]*Institut für Anorganische Chemie, Georg-August-Universität, Göttingen, Germany*
[c]*Department of Chemistry, Aarhus University, Denmark*

Received 26 January 2007; received in revised form 24 April 2007; accepted 26 April 2007
Available online 13 May 2007

Abstract

The compressibilities of disordered pyrochlores $NaCaMg_2F_7$ and $NaCdZn_2F_7$ (both $Fd\bar{3}m$, $Z = 8$) have been studied with X-ray single-crystal and powder diffraction using diamond anvil cells to 6.5 and 9.0 GPa at room temperature, respectively. The compressibility data are fitted with the Murnaghan equations of state. The zero-pressure bulk modulus B_0 and the unit-cell volume at ambient pressure V_0 (for the fixed first pressure derivative of the bulk modulus $B' = 4.00$) are equal to 83(2) GPa and 1107.12(1.33) Å^3 for $NaCdZn_2F_7$ and to 83(5) GPa and 1079.29(2.62) Å^3 for $NaCaMg_2F_7$. Upon decreasing the unit-cell volume, the positional x parameter of the F(2) atom increases in $NaCdZn_2F_7$ but is constant in $NaCaMg_2F_7$. In both cases, the (Na,Cd)F_8 and (Na,Ca)F_8 cubes become more regular and are softer than the ZnF_6 and MgF_6 octahedra, respectively. Both materials are structurally stable at least to the respective highest pressures reached in this study. These observations are compared to the high-pressure behavior of oxide pyrochlores.

Keywords: Pyrochlores

1. Introduction

The ideal pyrochlore structure ($Fd\bar{3}m$, $Z = 8$) has the general formula $A_2B_2X_6X'$ (A = Na, Ca, Sr, Mg, etc.; B = Nb, Ta, Ti, Fe, etc.; X and X' = O, F, or OH^-) [1–3]. The cations at the A site are coordinated by eight anions (six anions X and two anions X'), while the cations at the B site are six-fold coordinated to the anions X. The Wyckoff sites for the atoms A, B, X', and X are 16d (1/2,1/2,1/2), 16c (0,0,0), 8b (3/8,3/8,3/8), and 48f (x,1/8,1/8), respectively. The substitution of different cations at the A and B sites is possible. In the fluoride group, only three representatives with the general composition $A^{1+}A'^{2+}B_2^{2+}F_7$ are known. These are $NaSrMg_2F_7$ [4], $NaCaMg_2F_7$ [5], and $NaCdZn_2F_7$ [6] (Fig. 1), in which the atoms Na/Sr, Na/Ca, and Na/Cd, respectively, are randomly distributed over the A sites.

Most of the oxide pyrochlores amorphize or decompose at high pressures and the critical pressures for the onset of amorphization depend on the ionic radii of the substituted cations [7–9]. For instance, the structural stability of the crystalline state in the compounds $A_2Ti_2O_7$ increases with decreasing ionic radii at the A site. On the other hand, the stability is also enhanced with increasing ionic radii at the B site [8]. Also, in the series $Tb_2Ti_2O_7$, Tb_2TiSnO_7, and $Tb_2Sn_2O_7$ the bulk modulus increases 175 GPa → 202 GPa → 210 GPa, respectively [8]. $Cd_2Nb_2O_7$ decomposes at 4 GPa [9]. A subtle distortion leading to symmetry lowering of the cubic pyrochlore lattice in $Gd_2Ti_2O_7$ at 9 GPa, well below the amorphization at 38 GPa [7] was also reported [10].

The crystallographic information about the pressure dependence of the structural distortions in oxide pyrochlores has been provided by Kumar et al. [8], Saha et al. [10], and Ishikawa et al. [11]. The fractional coordinate of the oxygen atom (the atom X in the crystallochemical formula $A_2B_2X_6X'$) at the site (x,1/8,1/8) either is constant and independent of the cations [8,10] or increases with

*Corresponding author. Fax: +34 94 601 35 00.
E-mail address: andrzej@wm.lc.ehu.es (A. Grzechnik).

0022-4596/$ - see front matter © 2007 Elsevier Inc. All rights reserved.
doi:10.1016/j.jssc.2007.04.026

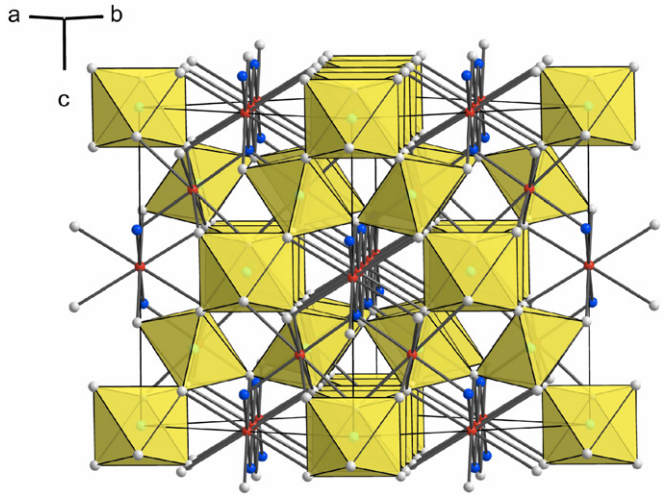

Fig. 1. Crystal structure of $NaCdZn_2F_7$ ($Fd\bar{3}m$, $Z = 8$). The (Na,Cd), Zn, F(1), and F(2) atoms are represented by cyan, black, blue, and light gray symbols, respectively.

increasing pressure [11]. This coordinate is constant regardless the substitution of Ti with Sn in the compounds $Tb_2Ti_2O_7$, Tb_2TiSnO_7, and $Tb_2Sn_2O_7$ [8]. On the other hand, the increase of the x parameter in $Nd_2Mo_2O_7$ with the physical (hydrostatic) pressure is analogous to its increase with the chemical pressure through substitution of the Nd atom (the ionic radius 1.109 Å) with the atoms Sm (1.079 Å), Gd (1.053 Å), and Dy (1.027 Å) [11].

The correlation between the high-pressure behavior of the pyrochlore structure and the substitution of the cations is likely to exist not only in oxides. This project has thus aimed to elucidate the changes in structural parameters and ordering of main group and transition metals in fluoride pyrochlores $NaCaMg_2F_7$ and $NaCdZn_2F_7$ upon compression at room temperature. We have carried out our investigations using X-ray single-crystal and powder diffraction in diamond anvil cells.

2. Experimental

Polycrystalline samples of $NaCaMg_2F_7$ and $NaCdZn_2F_7$ were studied with X-ray powder diffraction at room temperature and ambient pressure on the Diff beamline at the ANKA Synchrotron Light Source in Karlsruhe. The measurements were carried out in the Bragg–Brentano geometry ($\lambda = 0.9497$ Å) with the angular step of 0.004°. The data were normalized with the monitor counting rates.

High-pressure X-ray powder diffraction studies were performed at the beamline D3 in HASYLAB (Hamburg, Germany). Finely ground samples were loaded into a DXR-6 (Diacell) diamond anvil cell for angle-dispersive powder X-ray diffraction measurements to about 9.0 GPa with monochromatic radiation at 0.4 Å. The slits of the monochromator were closed to about 50×50 μm. The diamond cell was optically aligned on the four-circle diffractometer. The data were collected on a MAR-CCD-165 detector. The images were integrated with the program FIT2D [12] to yield intensity versus 2θ diagrams. A fluorite powder was added as an internal standard for the 2θ calibration at each pressure through the CaF_2 equation of state [13].

A series of X-ray single-crystal intensity measurements were carried out at high pressure on a crystal (approximately $50 \times 50 \times 30$ μm) of $NaCdZn_2F_7$ using a diffractometer IPDS-I (STOE) with Mo$K\alpha$ radiation collimated at the crystal to 0.5 mm. The diamond cell was of the Ahsbahs type (the opening angle of 90°) [14]. The diamond culets (600 μm) were modified by laser machining so that the angle between them and the tapered parts of the diamonds was 40°. A 250 μm hole was drilled into a stainless steel gasket preindented to a thickness of 80 μm. The intensities at 0.78, 3.20, and 4.54 GPa were collected upon compression, while the intensities at 2.13 GPa were collected on decompression from 4.54 GPa. The data were measured in two different orientations of the diamond anvil cell rotated by 90° around the incident X-ray beam. For each of the orientations, the exposures were performed in the angular ranges $48° \leqslant \varphi \leqslant 132°$ and $228° \leqslant \varphi \leqslant 312°$. The intensities were integrated simultaneously with three orientation matrices, corresponding to the crystal of $NaCdZn_2F_7$ and to two diamonds. This procedure allowed to exclude any reflections from the pyrochlore that were overlapped with the reflections from the diamonds.[1] The integrated intensities were corrected for absorption using the STOE software.[2] Due to the particular semi-spherical cut of the diamonds, no absorption correction was necessary for the diamond anvils.

During both powder and single-crystal measurements, the ruby luminescence method [15] was implemented for pressure calibration and the 1:4 mixture of ethanol:methanol was used as a hydrostatic pressure medium. The error in the pressure determination was about 0.1 GPa.

3. Results and discussion

The room-temperature ambient-pressure lattice parameters and unit-cell volumes of $NaCdZn_2F_7$ and $NaCaMg_2F_7$ pyrochlores from the powder data measured at ANKA are $a_0 = 10.34657(3)$ Å, $V_0 = 1107.62(1)$ Å^3, and $a_0 = 10.2574(1)$ Å, $V_0 = 1079.22(1)$ Å^3, respectively. The X-ray powder patterns collected at high pressures (most of them contain reflections due to the gasket material as the optical alignment of the diamond cell is not exactly precise) provide an evidence that both $NaCdZn_2F_7$ and $NaCaMg_2F_7$ are structurally stable to 9.0 and 6.5 GPa, respectively, with no indication either for ordering of the cations or for structural distortions. The compressibility data shown in Fig. 2 were extracted using the program Chekcell for the unit-cell refinement [16]. They could be fitted with the Murnaghan equations of state to give the zero-pressure bulk modulus B_0 and the unit-cell volume at ambient pressure V_0 (for the fixed first pressure derivative of the bulk modulus $B' = 4.00$) equal to 83(2) GPa and

[1] TWIN program. STOE & Cie GmbH, Darmstadt.
[2] X-shape program. STOE & Cie GmbH, Darmstadt.

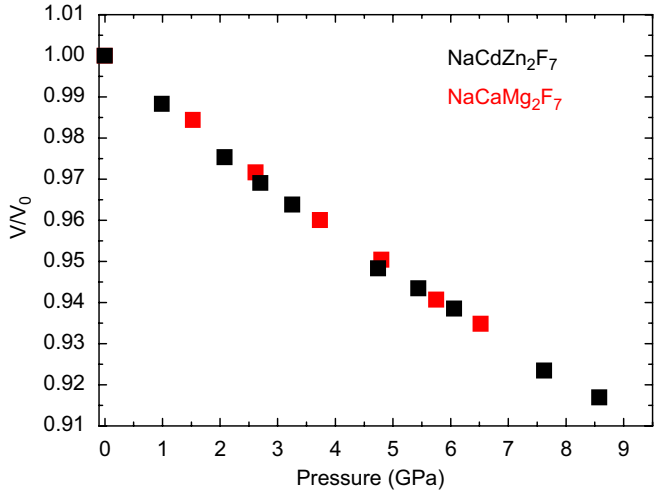

Fig. 2. Pressure dependence of reduced unit-cell volumes in $NaCdZn_2F_7$ (black symbols) and $NaCaMg_2F_7$ (red symbols).

Table 1
Experimental details for single-crystal refinements of $NaCdZn_2F_7$

Pressure (GPa)	0.78	2.13	3.20	4.54
Crystal data				
a (Å)	10.313(5)	10.261(5)	10.222(5)	10.176(5)
V (Å^3)	1096.9(16)	1080.4(16)	1068.1(16)	1053.7(16)
ρ (g/cm^3)	4.8325	4.9064	4.9627	5.0304
μ (mm^{-1})	12.852	13.048	13.198	13.378
G_{iso}	0.033(7)	0.050(7)	0.044(8)	0.042(6)
Data collection				
No. measured refl.	333	313	312	308
No. unique refl.	27	23	24	23
No. observed refl.[a]	20	20	20	21
$R(\text{int})_{obs/all}$ (%)	3.54/3.54	3.23/3.23	3.80/3.80	4.11/4.11
$\sin(\theta)/\lambda$	0.557023	0.564522	0.554909	0.562379
Refinement[b]				
R_{obs}	2.25	2.39	2.99	2.71
wR_{obs}	3.46	3.00	3.35	2.51
R_{all}	4.95	2.92	3.93	3.39
wR_{all}	3.69	3.05	3.42	2.62
GoF_{all}	2.50	2.35	2.44	2.01
GoF_{obs}	2.80	2.53	2.67	2.03
No. parameters	3	3	3	3

[a]Criterion for observed reflections is $|F_{obs}| > 3\sigma$; range of hkl: $0 \leqslant h \leqslant 6$, $0 \leqslant k \leqslant 8$, $1 \leqslant l \leqslant 10$.

[b]All agreement factors are given in %, weighing scheme $1/[\sigma^2(F_{obs}) + (0.01F_{obs})^2]$.

1107.12(1.33) Å^3 for $NaCdZn_2F_7$ and 83(5) GPa and 1079.29(2.62) Å^3 for $NaCaMg_2F_7$.

The structural refinements of the single-crystal data on $NaCdZn_2F_7$ collected at high pressures were performed with the program JANA2000 [17]. The parameters are presented in Tables 1 and 2.[3] The structural model ($Fd\bar{3}m$, $Z = 8$) consisted of the (Na,Cd), Zn, and F(1) atoms at the positions (0.5,0.5,0.5), (0,0,0), and (0.375,0.375,0.375), respectively [6,18]. The F(2) atom is at the position (x,0.125,0.125) (Table 2). The two data sets for two different orientations of the diamond anvil cell were refined together with a common scale factor. All the weak reflections ($I < 3\sigma$) overlapping with the Debye–Scherrer rings of the gasket material were excluded from the refinement as their intensities were not correct. We encountered problems with the refinement of the displacement parameters for all the atoms, which we attribute to the limited resolution of the data, i.e., the $\sin(\theta)/\lambda$ limit (Table 1) is relatively low arising from the small opening angle in our diamond anvil cell. For this reason, all the anisotropic displacement parameters were taken from reference [6] and fixed. An isotropic Gaussian extinction correction (G_{iso}) was also applied [19].

[3]Further details of the crystallographic investigations can be obtained from the Fachinformationszentrum Karlsruhe, D-76344 Eggenstein-Leopoldshafen, Germany, on quoting the depository numbers CSD 418065–418069.

Table 2
The x coordinate of the fluorine atom F(2) from single-crystal refinements of $NaCdZn_2F_7$

Pressure (GPa)	0.78	2.13	3.20	4.54
z	0.332(1)	0.335(1)	0.334(1)	0.336(1)

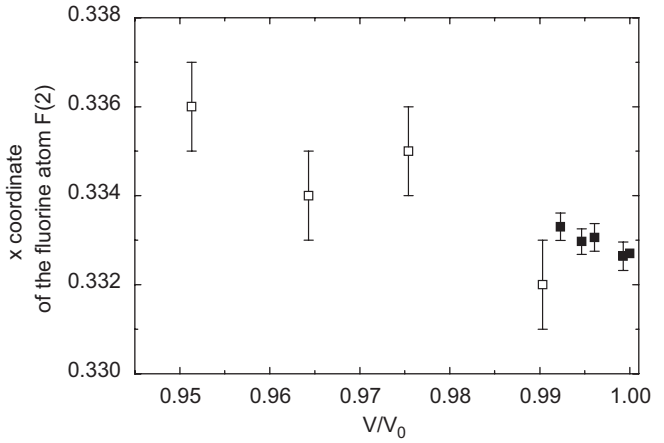

Fig. 3. Volume dependence of the x coordinate of the F(2) atom in $NaCdZn_2F_7$. Open and full symbols stand for the high-pressure (this study) and low-temperature [18] data. The data point at room temperature and ambient pressure ($V/V_0 = 1.0$) is taken from Ref. [6]. The error bars are shown when larger than the size of the data points.

The pressure dependence of the x coordinate of the fluorine atom F(2) in $NaCdZn_2F_7$ shown in Table 2 is a measure of a distortion from the ideal fluorite type ($x = 0.375$), for which the coordination around the (Na,Cd) site would be a regular cube and the Zn atom would possess the trigonal antiprismatic coordination. When $x = 0.3125$, the Zn atom would be at the center of a regular octahedron, while the (Na,Cd) atoms would have the 6+2 scalenohedral coordination. To correlate the effects of temperature and pressure on the crystal structure, all the structural parameters could be plotted as a function of a unit-cell volume normalized to the unit-cell

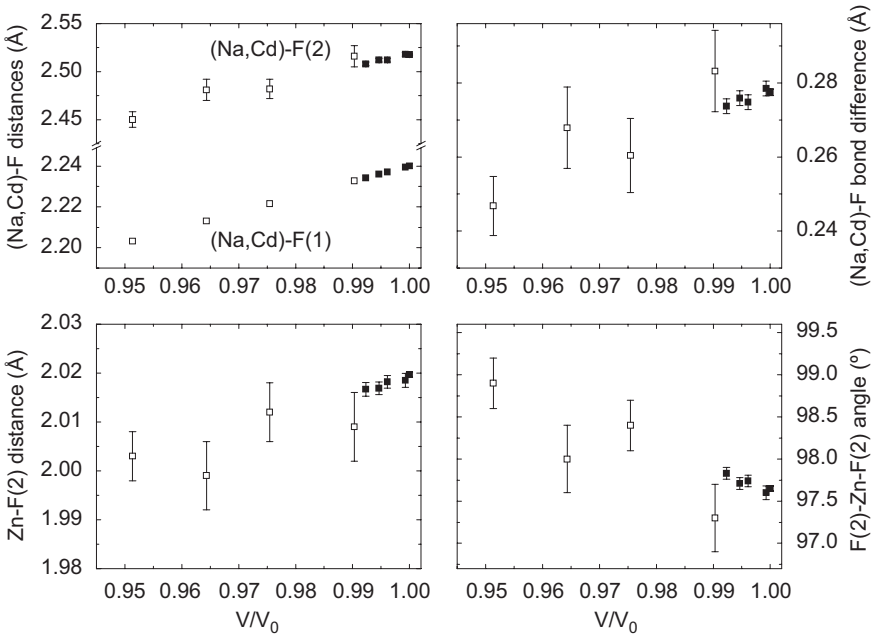

Fig. 4. Volume dependence of selected structural parameters in $NaCdZn_2F_7$. Open and full symbols stand for the high-pressure (this study) and low-temperature [18] data. The data points at room temperature and ambient pressure ($V/V_0 = 1.0$) are taken from Ref. [6]. The error bars are shown when larger than the size of the data points.

volume at room temperature and atmospheric pressure, $V_0 = 1107.62(1)\,\text{Å}^3$. Fig. 3 shows the unit-cell volume dependence of the x coordinate when the $NaCdZn_2F_7$ crystal is compressed at room temperature (this study) and when it is cooled down at atmospheric pressure [18]. The volume change on cooling from 298 to 100 K at ambient conditions [18] corresponds to compressing the material to about 0.6 GPa at room temperature, according to the equation of state given above. The x coordinate has the same behavior at high pressures and low temperatures. Fig. 3 clearly demonstrates that the distortion of the ideal fluorite type diminishes upon decreasing the unit-cell volume. Consequently, the $(Na,Cd)F_8$ cubes become more regular and the ZnF_6 octahedra become more distorted along the three-fold $\langle 1\,1\,1 \rangle$ axis as also seen from the volume dependence of the (Na,Cd)–F bond length differences and F(2)–Zn–F(2) angles (Fig. 4). Our data in Fig. 5 show that the $(Na,Cd)F_8$ polyhedral volume [20] is more sensitive to the changes to the bulk unit-cell volume than the volume of the ZnF_6 octahedra.

The powder pattern of $NaCaMg_2F_7$ collected at 5.85 GPa was refined with the Rietveld method using the program JANA2000 [17] (Table 3 and Fig. 6). The structural model was like the one for single-crystal refinements of the high-pressure data for $NaCdZn_2F_7$. The isotropic displacements parameters for all the atoms were taken from Ref. [5] and fixed. Overall, the refined variables were: the x atomic position of the F(2) atom, lattice parameters of CaF_2 and $NaCaMg_2F_7$, two scale factors, eight terms of the Legendre polynomial background, and two sets of GP, LX, and LY profile parameters for the two components.

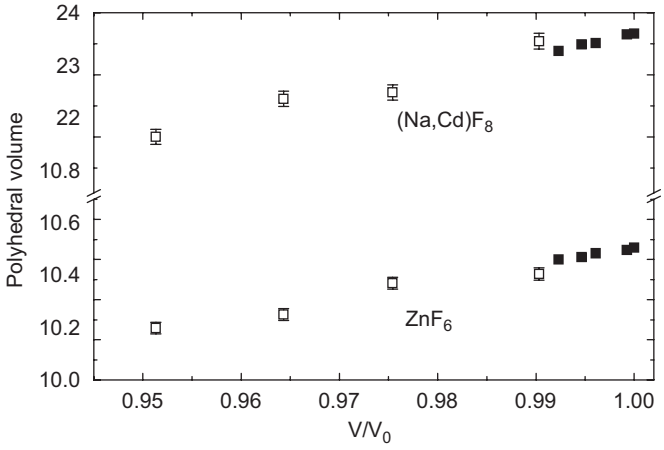

Fig. 5. Volume dependence of polyhedral volumes in $NaCdZn_2F_7$. Open and full symbols stand for the high-pressure (this study) and low-temperature [18] data. The data points at room temperature and ambient pressure ($V/V_0 = 1.0$) are taken from Ref. [6]. The error bars are shown when larger than the size of the data points.

The structural data for $NaCaMg_2F_7$ at 5.85 GPa are displayed in Table 4. Unlike in $NaCdZn_2F_7$, the x coordinate is practically independent of pressure. Hence, the interatomic distances, angles, polyhedral volumes and distortions scale with the pressure dependence of the unit-cell volume (Fig. 2). In this case, the fact that the $(Na,Ca)F_8$ cubes become more regular and are softer than the MgF_6 octahedra upon compression is entirely due to the bulk volume change.

The high-pressure behavior of interatomic distances and polyhedral volumes in the pyrochlore structures of

Table 3
Experimental details for a Rietveld refinement of $NaCaMg_2F_7$

Pressure (GPa)	5.85
Crystal data	
a (Å)	10.048(1)
V (Å^3)	1014.3(3)
ρ (g/cm^3)	3.2033
Data collection	
No. observed refl.	32
$\sin(\theta)/\lambda$	0.533654
Refinement[a]	
R_{obs}	7.80
wR_{obs}	7.52
R_{all}	10.70
wR_{all}	8.09
No. parameters	2

[a]All agreement factors are given in %.

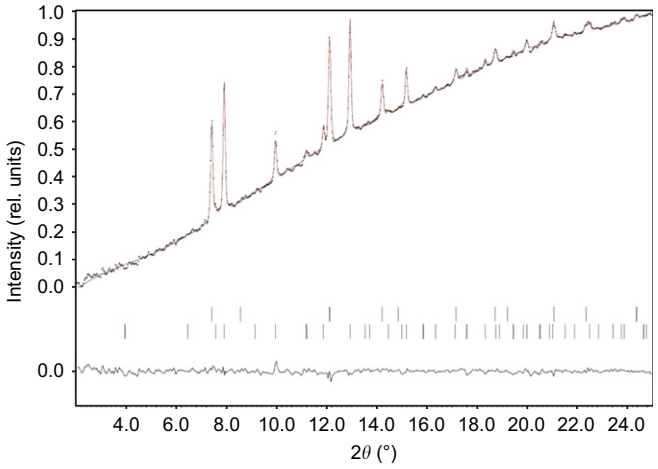

Fig. 6. Observed, calculated, and difference X-ray powder patterns for $NaCaMg_2F_7$ at 5.85 GPa ($\lambda = 0.4$ Å). Vertical markers indicate Bragg reflections of CaF_2 (top) and $NaCaMg_2F_7$ (bottom).

Table 4
Structural details obtained from a Rietveld refinement of $NaCaMg_2F_7$

Pressure (GPa)	0.0001 [5]	5.85
x coordinate	0.3270(1)	0.329(2)
(Na,Ca)–F(1) distance (Å)	2.2215(1)	2.18
(Na,Ca)–F(2) distance (Å)	2.5375(1)	2.47(1)
Difference in (Na,Ca)–F distances (Å)	0.3160(2)	0.29(1)
Mg–F(2) distance (Å)	1.9788(6)	1.946(8)
F(2)–Mg–(F2) angle (deg)	95.6[a]	96.4(5)
Polyhedral volume (Na,Ca)F_8 (Å^3)	24.0(1)	22.2(1)
Polyhedral volume MgF_6 (Å^3)	10.17(2)	9.63(2)

[a]Calculated from the data of reference [5] (the error is not known).

$NaCdZn_2F_7$ and $NaCaMg_2F_7$ could also be analyzed in terms of bond compressibilities and bond valencies, as weak bonds would be expected to have low valence and be more compressible [21,22]. Based on the data

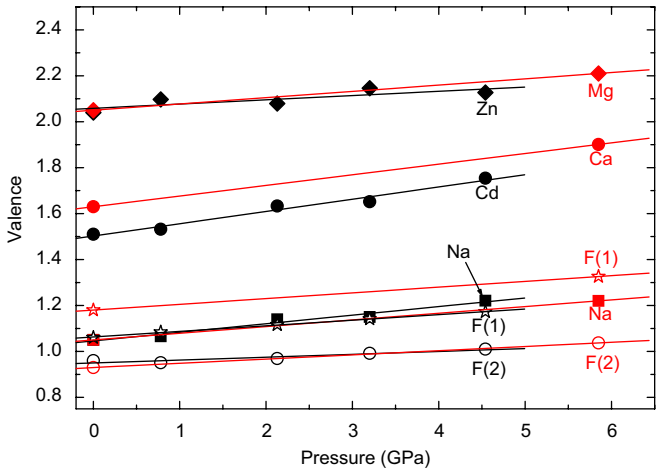

Fig. 7. Pressure dependence of bond valence sums. Black and red symbols stand for the sums of the atoms in $NaCdZn_2F_7$ and $NaCaMg_2F_7$, respectively. Solid lines are linear fits to the data. The points at atmospheric conditions are taken for Refs. [6] and [5], respectively.

presented in reference [6] and this study, the compressibilities[4] of the (Na,Cd)–F(1), (Na,Cd)–F(2), and Zn–F(2) bonds in $NaCdZn_2F_7$ are 3.6×10^{-3}, 6.0×10^{-3}, and 1.8×10^{-3} GPa^{-1}, respectively. The compressibilities of the (Na,Ca)–F(1), (Na,Ca)–F(2), and Mg–F(2) bonds in $NaCaMg_2F_7$ (reference [5] and this study) are 3.2×10^{-3}, 4.6×10^{-3}, and 2.9×10^{-3} GPa^{-1}, respectively. In both structures, the least compressible distances are the Zn–F(2) and Mg–F(2) bonds, respectively. The effect of increased pressure to about 6.0 GPa on all the respective R_0 parameters to calculate the bond valences [21] in $NaCdZn_2F_7$ and $NaCaMg_2F_7$ is negligible so that the standard R_0 values could used for the present data [23]. For the A sites, a relation of the monovalent to the divalent cation is 1:1, leading to an ideal bond valence sum of 1.5 at atmospheric conditions. As can be seen from Fig. 7, the resulting values of bond valence sums for the Zn and Mg atoms in $NaCdZn_2F_7$ and $NaCaMg_2F_7$ are less sensitive to increased pressure than the sums for the atoms at the A sites, especially than the sums of the Cd and Ca atoms, respectively. This observation correlates very well with the fact that the (Na,Cd)F_8 and (Na,Ca)F_8 cubes are softer than the ZnF_6 and MgF_6 octahedra, respectively.

4. Concluding remarks

Our experimental data obtained with X-ray single-crystal and powder diffraction show that both pyrochlores $NaCdZn_2F_7$ and $NaCaMg_2F_7$ ($Fd\bar{3}m$, Z = 8) are structurally stable to 9.0 and 6.5 GPa, respectively, with no indication either for ordering of the cations or for structural distortions.

In the oxide pyrochlores, the bulk moduli that are larger than 170 GPa depend on the ionic radii [7,8,10]. It is quite

[4]The bond compressibility is defined as $\beta_{ij} = (-1/R_{ij})(dR_{ij}/dP)$.

likely that the ionic radius dependence of the bulk modulus also holds for fluoride pyrochlores. The same values of the moduli for $NaCaMg_2F_7$ and $NaCdZn_2F_7$ of 83 GPa could thus be explained with the fact that the effective ionic radii for the cations Ca^{2+} and Cd^{2+} (the coordination number 8) as well as for the cations Mg^{2+} and Zn^{2+} (the coordination number 6) are nearly identical, respectively: 1.12 Å (Ca^{2+}) and 1.10 Å (Cd^{2+}), 0.89 Å (Mg^{2+}) and 0.90 Å (Zn^{2+}) [24].

In this study, we show that, upon decreasing the unit-cell volume due to compression at room temperature and/or thermal contraction at atmospheric conditions, the positional parameter of the F(2) atom increases in $NaCdZn_2F_7$ but is constant in $NaCaMg_2F_7$. In both cases, the $(Na,Cd)F_8$ and $(Na,Ca)F_8$ cubes become more regular and are softer than the ZnF_6 and MgF_6 octahedra, respectively. As a consequence, we conclude that the polyhedral distortions and structural deviations from the ideal fluorite type in fluoride pyrochlores are dependent not only on the positional coordinate of the F(2) atom but also on the unit-cell volume. At present, no more data on a possible correlation between the high-pressure behavior of this coordinate in fluorides and the cationic substitution is available.

Acknowledgments

This work has been financially supported by the Ministerio de Ciencia y Tecnología and the Gobierno Vasco. The synchrotron experiments at the ANKA Synchrotron Light Source in Karlsruhe have been supported by the European Community-Research Infrastructure Action under the FP6: Structuring the European Research Area, Integrating Activity on Synchrotron and Free Electron Laser Science (IA-SFS, RII3-CT-2004-506008). The high-pressure synchrotron data have been collected during the I-20060049 EC beamtime in HASYLAB (Hamburg). We also thank Stephen Doyle and Alberto Herrero (TEKNIKER, Eibar) for their help with the experiments at ANKA and with preparations of the measurements in our high-pressure laboratory in Bilbao, respectively.

References

[1] N.P. Raju, J.E. Greedan, M.A. Subramanian, C.P. Adams, T.E. Mason, Phys. Rev. B 58 (1998) 5550;
P. Dahlke, J. Pebler, D. Babel, Z. Anorg. Allg. Chem. 631 (2005) 115.
[2] M.J. Harris, M.P. Zinkin, Mod. Phys. Lett. B 10 (1996) 417;
T. Zeiske, M.J. Harris, M.P. Zinkin, Physica B 234 (1997) 766;
M.P. Zinkin, M.J. Harris, T. Zeiske, Phys. Rev. B 56 (1997) 11786.
[3] K. Friese, J.-Y. Gesland, A. Grzechnik, Z. Kristallogr. 220 (2005) 614.
[4] F. Kubel, B. Dundjerski, Z. Anorg. Allg. Chem. 627 (2001) 1589.
[5] E.A. Oliveira, I. Guedes, A.P. Ayala, J.-Y. Gesland, J. Ellena, R.L. Moreira, M. Grimsditch, J. Solid State Chem. 177 (2004) 2943.
[6] K. Friese, A. Grzechnik, W. Morgenroth, G. Buth, S. Doyle, J.-Y. Gesland, Acta Crystallogr. E 61 (2005) i182–i184.
[7] F.X. Zhang, B. Manoun, S.K. Saxena, C.S. Zha, Appl. Phys. Lett. 86 (2005) 181906.
[8] R.S. Kumar, A.L. Cornelius, M.F. Nicol, K.C. Kam, A.K. Cheetham, J.S. Gardner, Appl. Phys. Lett. 88 (2006) 031903.
[9] F.X. Zhang, J. Lian, U. Becker, R.C. Ewing, L.M. Wang, L.A. Boatner, J. Hu, S.K. Saxena, Phys. Rev. B 74 (2006) 174116.
[10] S. Saha, D.V.S. Muthu, C. Pascanut, N. Dragoe, R. Suryanarayanan, G. Dhalenne, A. Revcolevschi, S. Karmakaran, S.M. Sharma, A.K. Sood, Phys. Rev. B 74 (2006) 064109.
[11] H. Ishikawa, Sh. Xu, Y. Moritomo, A. Nakamura, Phys. Rev. B 70 (2004) 104103.
[12] A.P. Hammersley, S.O. Svensson, M. Hanfland, A.N. Fitch, D. Häusermann, High Press. Res. 14 (1996) 235.
[13] R.J. Angel, J. Phys.: Condens. Matter 5 (1993) L141.
[14] H. Ahsbahs, Z. Kristallogr. 9 (Suppl) (1995) 42;
H. Ahsbahs, Z. Kristallogr. 219 (2004) 305.
[15] G.J. Piermarini, S. Block, J.D. Barnett, R.A. Forman, J. Appl. Phys. 46 (1975) 2774;
H.K. Mao, J. Xu, P.M. Bell, J. Geophys. Res. 91 (1986) 4673.
[16] J. Laugier, B. Bochu 〈http://www.inpg.fr/LMGP〉.
[17] V. Petricek, M. Dusek, L. Palatinus, Jana200. The Crystallographic Computing System, Institute of Physics, Praha, Czech Republic, 2000.
[18] A. Grzechnik, R. Kaindl, K. Friese, J. Phys. Chem. Solids 68 (2007) 382.
[19] P.J. Becker, P. Coppens, Acta Crystallogr. A 30 (1974) 129.
[20] T. Balic-Zunic, I. Vickovic, J. Appl. Cryst. 29 (1996) 305.
[21] I.D. Brown, P. Klages, A. Skowron, Acta Crystallogr. B 59 (2003) 439.
[22] J. Zhao, N.L. Ross, R.J. Angel, Acta Crystallogr. B 60 (2004) 263.
[23] I.D. Brown. Accumulated list of bond valence parameters, 2002 〈http://ccp14.ac.uk/ccp/web-mirrors/i_d_brown〉
[24] R.D. Shannon, Acta Crystallogr. A 32 (1976) 751.